Characteristics of Fluid Flow in the Fluidized Bed Shell and Tube Type Heat Exchanger with Corrugated Tubes

Soo Whan Ahn[†] , Sung Taek Bae[*], Myoung Ho Kim[**]

School of Mechanical & Aerospace Engineering, Gyeongsang National University,
Institute of Marine Industry, Tongyong 650-160, Korea
[*]Taekeon Co., Ltd, 419-12 Sagok Sadung, Geoje 656-880, Korea
[**]Marine Engineering Dpt, Graduate School, Gyeongsang National University, Tongyong 650-160, Korea

ABSTRACT: An experimental study was carried on the characteristics of fluid flow and heat transfer in a fluidized bed shell-and-tube type heat exchanger with corrugated tubes. Seven different solid particles having same volume were circulated in the tubes. The effects of various parameters such as water flow rates, particle geometries and materials, and geometries of corrugated tubes on relative velocities and drag coefficients were investigated. The present work showed that the drag force coefficients of particles in the corrugated tubes were usually lower than those in the smooth tubes, meanwhile the relative velocities between particles and water in the corrugated tubes were little higher than those in the smooth tubes except the particles of glasses.

―――――――― Nomenclature ――――――――

A : contact area [m^2]

C_d : drag coefficient

D : diameter [m]

D_h : hydraulic diameter of test section [m]

D_e : envelope diameter, see Fig. 1 [m]

D_b : bore, see Fig. 1 [m]

D_{oi} : inner diameter of outer tube [m]

D_{vi} : volume-based corrugated tube inner diameter [m]

D_{vo} : volume-based corrugated tube outer diameter [m]

e : height of trough, $(D_e - D_b)/2$ [m]

e^* : dimensionless depth of trough, e/D_{vo}

F_b : buoyancy force [N]

F_d : drag force [N]

F_g : gravity force [N]

g : gravity acceleration [m/s^2]

P : trough pitch [m]

P^* : dimensionless trough pitch, P/D_{vo}

Re$_1$: Reynolds number based on solid particle, $(u_b D_h)/\nu$

U : fluid velocity [m/s]

U_r : relative velocity, $U - U_s$ [m/s]

U_s : particle velocity [m/s]

θ : corrugation helix angle, $\tan^{-1}(\pi D_{vo}/NP)$

θ^* : $\theta/90$

ν : kinematic viscosity [m^2/s]

† Corresponding author
  Tel.: +82-55-640-3125; fax: +82-55-640-3128
  E-mail address: swahn@gaechuk.gsnu.ac.kr

1. Introduction

Different concepts to mitigate fouling of heat

exchangers have been developed ranging from identifying low fouling operating conditions of heat exchangers to making use of highly specialized equipment such as tube inserts and fluidized bed heat exchangers. For proper design of circulating fluidized bed heat exchanger, it is important to know the effect of design and operating parameters on the bed-to-wall heat transfer coefficient. At present there is a dearth of mechanistic models for predicting these effects. The effects of micro-sized particles below the diameter of 200 μm on heat transfer coefficients in the fluidized bed heat exchanger were studied by Bowen and Epstein,[1] Basu and Nag,[2] Sjollema and Busscher,[3] and Adomeit and Renz.[4] Basu and Nag[2] measured the heat transfer coefficients for different superficial velocities and solid circulation rates and particle sizes. They could conclude that bed-to-wall heat exchange increases with increasing suspension density; but it decreases if the fluidization velocity is increased while keeping the recycling rate constant. Adomeit and Renz[4] recently developed a numerical method to predict particle transport in turbulent and non-isothermal flow which shows reasonable agreement with experimental data. The experimental investigation by Adomeit and Renz[4] showed that increasing flow rates lead to a decrease of the effective heat transfer rate to the heat exchanger surface. This is in contradiction to the general assumption that increasing flow rates enhance energy transport as deduced from general concept. However, the observed behaviour can be explained by hydrodynamic lift forces acting on the particle, caused by both flow confinement and shear in the vicinity of the wall.

Previous investigations of particle detachment have either focused on the effect of drastically increasing flow shear rates[5] or on the influence of chemical compounds added for cleaning purposes.[6] Fluidized bed heat exchangers with circulating solid particles of more than 2 mm diameter have been studied by Hatch and Weth,[7] Rautenbach and Kollbach,[8] Kollbach et al.,[9] Tianqing,[10] and Lee et al.[11] Hatch and Weth[7] developed the fluidized bed heat exchangers for brine heating and heat recovery in multistage flash evaporators for seawater desalination. And Rautenbach and Kollbach[8] have firstly studied the characteristics of heat transfer in the fluidized bed heat exchangers in connection with wastewater evaporation in 1978. Lee et al.[11] investigated on the pressure loss, the heat transfer and the fouling characteristics of a particulate flow of the 3.0 mm-diameter-glass beads. The particles augmented the heat transfer at the region of velocities lower than 1.0 m/s. In this range, the heat transfer coefficient slightly increased as the particle volume fraction increased, and was almost independent of the flow velocity. The particles also increased the pressure loss at the region of flow velocities lower than 1.0 m/s. Above 1.0 m/s, however, the heat transfer coefficient and the pressure loss were essentially the same as those of pure water. And the researches for fluidized bed heat exchangers for incinerators and dryers have been done by Lee et al.,[12] Jun et al.,[13] Kim et al.[14] and Chun et al.[15]

These studies covered the pressure drop and heat transfer in the fluidized bed heat exchanger with smooth tubes. However, little information has been published on pressure drop and heat transfer in the fluidized bed heat exchanger with corrugated tubes. The main purpose of this study was to investigate the effects of solid particles circulated and corrugated tubes on relative velocities and drag coefficients in the heat exchanger for the use of fluidized bed heat exchanger with corrugated tubes. Seven different particles were used. The relative velocities of each particle, corresponding to the differences between fluid velocities and the particle velocities, were determined from the flow meter for fluid velocities and the CCD camera for particle velocities.

2. Experimental apparatus and test procedure

Figure 1 shows the detailed contour of corrugated tube in test section of tube side. The experimental apparatus was built to measure the pressure drop, heat transfer, and to perform a flow visualization test as shown in Fig. 2. The apparatus consists of a pump, valves, a water tank, two heat exchangers, a condensing coil, and a test section. The heat exchanger has the dimensions of 705 mm in height, 80.4 mm in shell diameter, and three different diameters in tubes (Table 1). Magnetic pump (190 W, PM-100 PD) was chosen because the wide
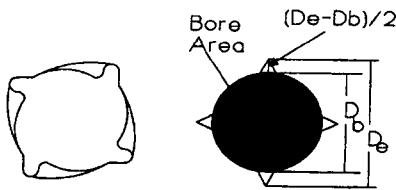
impeller spacing made solid particles or foreign materials pass through easily. Flow rate was controlled by valves which bypass a relevant amount of water back to the reservoir, and the fluid flow rate in the tube was measured with the cumulative type flow meter and a timer, of which the minimum range was 10 ml. Downstream of the test section, a condensing coil

Table 1   Test matrix for visualization measurements

	Inner tube (unit: mm)							
	D_s	D_{vi}	D_{vo}	P	N	e^*	P^*	θ^*
S_0	15.8	14.2	15.8					
T_1	15.8	13.88	15.48	7	1	0.045	0.45	0.91
T_2	15.8	13.97	15.57	10	1	0.045	0.64	0.89

D_s : Original smooth tube diameter

D_{vi} : Volume-based grooved tube inner diameter

D_{vo} : Volume-based grooved tube outer diameter

P : Flute or corrugation pitch

N : Number of flute or corrugation starts
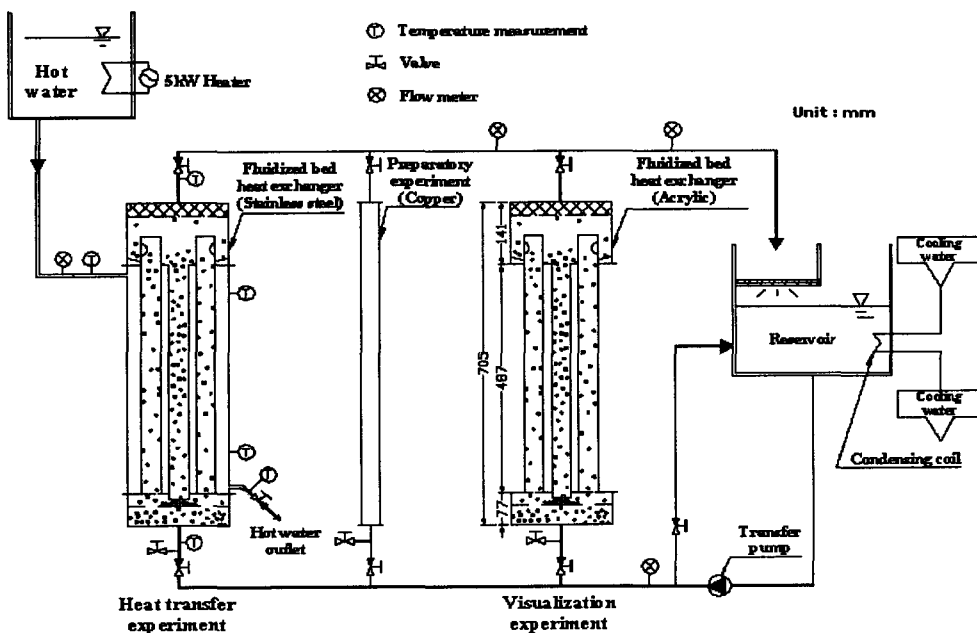
S_0 : Smooth tube

$T_{1,2}$: Spirally corrugated tube

Fig. 1   Volumetric diameter of a corrugated tube (see Table 1).

Fig. 2   Schematic diagram of experimental setup.

Table 2 Details of particles in fluidized bed

Classification	Material	Geometry	Dimension
Case (A)	glass	bead	3 mmΦ
Case (B)	Al	cylinder	2 mmΦ, 4.5 mmL
Case (C)	Al	cylinder	3 mmΦ, 2 mmL
Case (D)	steel	cylinder	2 mmΦ, 4.5 mmL
Case (E)	steel	cylinder	2.5 mmΦ, 2.88 mmL
Case (F)	Cu	cylinder	2.5 mmΦ, 2.88 mmL
Case (G)	sand	grain	3 mmΦ

was installed to maintain the constant temperature of circulating fluid at the entrance of test section. The visualization section for the preparatory experiment and the fluidized bed heat exchanger (right hand side in Fig. 2) were fabricated with a transparent acrylic material for easy accessibility of CCD camera. Particle flow was visualized by a CCD camera. Particle velocity was determined from the moving distance and elapsed time. The heat transfer test section (left hand side in Fig. 2) was made of stainless steel (SUS 304). Both the fluidized bed heat exchanger for heat transfer (left hand side) and that for visualization (right hand side) have same dimensions. Table 2 shows seven different particles used in experiment such as glass (bead, 3 mm dia.), aluminum (cylinder, 2 mm and 3 mm dia.), copper (cylinder, 2.5 mm dia.), steel (cylinder, 2 mm and 2.5 mm), and sand (grain, 2~4 mm dia.). All the particles have the same volume of 14 mm^3 except the sand. The U-type tube at inlet and the screen at exit prevented the particles from escaping out of the test section.

3. Results and discussion

Reynolds number was calculated from the measured flow rate based on the hydraulic diameter, D_h. It was noted that the corrugated tube does not have a circular cross section; therefore, a diameter that represented the average cross-sectional area of the corrugated tube was calculated from the volume of water (*Vol*)

required to fill a given length of tube as follows:

$$D_{vi} = \sqrt{\frac{4\,Vol}{\pi L}} \qquad (1)$$

The volumetric outside diameter, D_{vo}, which is the quantity of interest for the shell side, is calculated by adding twice the tube thickness to D_{vi}. To facilitate tube specification, a model geometric features such as D_b, D_e, P and N of Table 1 are shown Fig. 1. The detailed dimensions of corrugated tubes were represented in Table 1. The cross-sectional area was approximated as the sum of the clear bore area and the area within the corrugations, each corrugation being approximated as a triangle with the height equal to the corrugation depth. The force acting on the solid particle in the stream is shown in Fig. 3. Assuming the particle mass
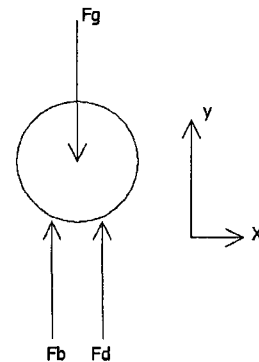

Fig. 3 Force acting on a solid particle.

becomes m_p, the gravity force (F_g) is given by:

$$F_g = m_p g \qquad (2)$$

The buoyancy force is attributed to density difference between the particle and the surrounding fluid, the buoyancy force (F_b) is obtained from the fluid mass (m_w) as follows:

$$F_b = m_w g \qquad (3)$$

And the drag force (F_d) means the resultant force in terms of viscosity acted by a particle and the surrounding fluid. From an usual definition of friction factor, the drag force becomes:

$$F_d = 0.5 \rho_w U_r^2 C_d A \qquad (4)$$

Here, U_r, C_d, and A represent relative velocity between a particle and stream fluid, frictional drag coefficient, and contact surface. In this study, Reynolds numbers are defined as equation (5). The Re_1 was used for the presentation of the drag coefficient results.

$$Re_1 = (U_r d_p)/v_w \qquad (5)$$

where v_w is the kinematic viscosity of fluid. The force balance yields the following equation:

$$-F_g + F_b + F_d = 0 \qquad (6)$$

Substituting gravity force (F_g), buoyancy force (F_b), and drag force (F_d) into equation (6), we obtain as:

$$-m_p g + m_w g + 0.5 \rho_w U_r^2 C_d A = 0 \qquad (7)$$

Drag coefficient (C_d) is calculated from equation (7).
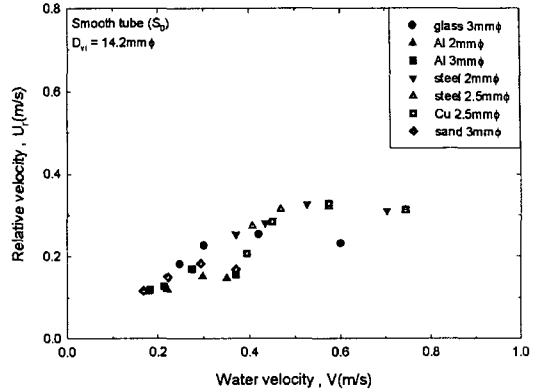

Fig. 4   Relative velocity for smooth tube.

Figure 4 represents the variations of relative velocities of seven solid particles against the fluid flow velocities in the smooth tube. The relative velocities, corresponding to the differences between fluid velocities and the particle velocities, were determined from the flow meter for fluid velocities and the CCD camera for particle velocities. The relative velocities of the copper particle of 2.5 mm diameter was the highest, while those of the aluminum particle of 2 mm diameter was the lowest. It is supposed that the higher the density of particle and closer geometry to spherical one are, the higher the relative velocity becomes because of the differences in gravity force and projected area under pressure. The relative velocities for all the particles usually increased, and then decreased with increasing water velocities. This phenomenon was more significant for the glass bead and copper. The increase in relative velocity means the decrease in fluid flow frictional resistance. The fluid flow frictional resistance is supposed to be a complex function of density, particle geometry, and surface area. Different material and geometry should influence the different particle flow velocity, and the effects of material and geometry on the particle flow velocity need further research.

The relative velocities in the corrugated tube were shown in Figs. 5 and 6. The relative velocities of particles except the glass in the
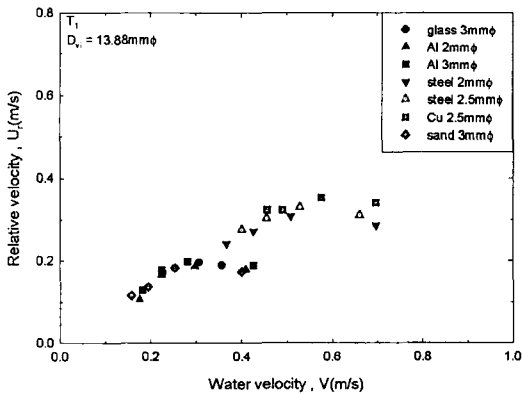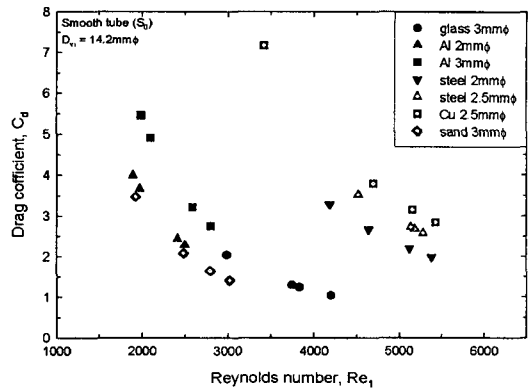
Fig. 5 Relative velocity for T_1.

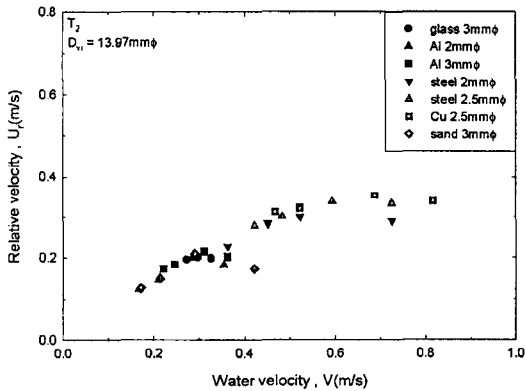Fig. 7 Drag coefficient for smooth tube.

Fig. 6 Relative velocity for T_2.
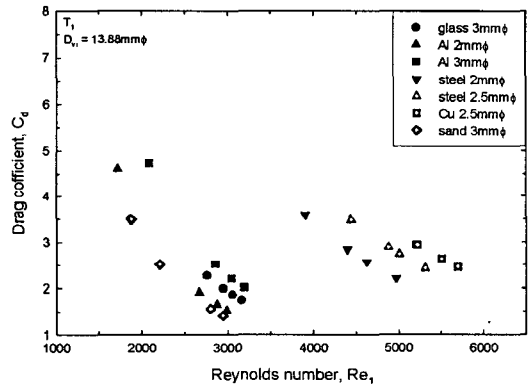

Fig. 8 Drag coefficient for T_1.

Fig. 9 Drag coefficient for T_2.

corrugated tube were higher than those in the smooth tube. It was probable that the trough of the corrugated tube intervened with flow of solid particle and increased the relative velocity. However, the relative velocity for the particle of glass in the corrugated tube was lower than that in the smooth tube. It was speculated that the glass, having the smooth spherical geometry without ridge, was less subject to the surface area resistance of corrugated tube, and the fluid flow velocity at the core of corrugated tube was higher than in the smooth tube on the condition of identical bulk velocity.

Figures 4 to 6 showed the relative velocity in the velocity range of solid particle colliding to the wall. Figures 5 to 6 have similar tendencies to Fig. 4. It means that the effect of
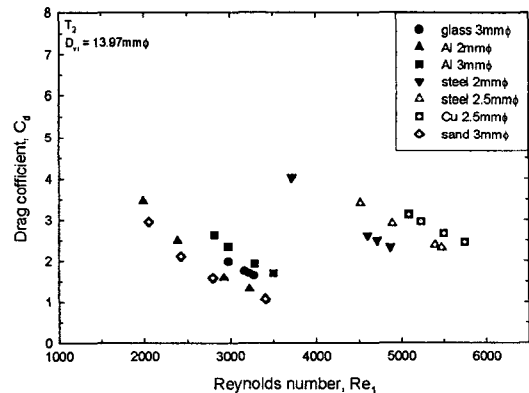
difference in the geometry of corrugated tube on variation of flow pattern should be insignificant. The relative velocity was the highest

in the copper, however, lowest in the aluminum because of difference in the particle density.

In the particle of steel, the relative velocity in the diameter of 2.5 mm was higher than that in the diameter of 2 mm. It was supposed that the particle diameter of 2.5 mm closer to the spherical geometry leads to higher fluid flow resistance. Figures 7 to 9 indicates drag coefficients against Reynolds number based on particle diameters and relative velocities. On the contrary to general expectation, the drag coefficients in the smooth tube of Fig. 7 were higher than those in the corrugated tube. It might be attributed to the fact that drag coefficients are inversely proportional to relative velocity (U_r) as shown in equation (7). In all figures the higher drag coefficients occurred at higher density materials. It was because the solid particles having higher densities have higher viscous resistances.

4. Conclusions

(1) The relative velocity in the copper particle of 2.5 mm diameter was the highest, and that in the aluminum particle of 2 mm diameter was the lowest. It is supposed that the higher the density of particle and closer geometry to spherical one are, the higher the relative velocity becomes because of the differences in gravity force and projected area under pressure.

(2) Except the glass particle, the relative velocities in the corrugated tubes were higher than those in the smooth tubes.

(3) The drag coefficients in the smooth tubes were higher than those in the corrugated tubes.

Acknowledgement

References

1. Bowen, B. D. and Epstein, N., 1979, Fine particle deposition in smooth parallel-plate channels, J. Coll. Interf. Sci., Vol. 72, pp. 81-97.
2. Basu, P. and Nag, P. K., 1987, An investigation into heat transfer in circulatiing fluidized beds, Int. J. of Heat and Mass Transfer, Vol. 30, No. 11, pp. 2399-2409.
3. Sjollema, J. and Busscher, H. J., 1988, Deposition of polystyrene latex particle toward polymethylmethacrylate in a parallel flow cell, J. Coll. Interf. Sci., Vol. 132, pp. 382-394.
4. Adomeit, P. and Renz, U., 1995 The influence of liquid flow rate on particle deposition and detachment, Proc. of Fouling Mitigation of Industrial Heat Exchange Equipment, An International Conference, San Luis Obispo, California, pp. 421-433.
5. Hubbe, M. A., 1985, Detachment of colloidal hydrous oxide spheres from flat solids exposed to flow: 2. Mechanisms of release, Coll. Surf., Vol. 16, pp. 249-270.
6. Kallay, N., Biskup, B., Tomic, M. and Matijevic, E., 1986, Particle adhesion and removal in model systems: X. The effect of electrolytes on particle detachment, J. Coll. Interf. Sci., Vol. 114(2), pp. 362-375.
7. Hatch, L. P. and Weth, G. G., 1970, Scale control in high temperature distillation utilizing fluidized bed heat exchanger, R & D Progress Report, No. 571.
8. Rautenbach, R. and Kollbach, J. 1986, New developments in fluidized bed heat transfer for preventing fouling, Swiss Chem., Vol. 8, No. 5, pp. 47-55.
9. Kollbach, J., Dahm, W. and Rautenbach, R., 1987, Continuous cleaning of heat exchanger with recirculating fluidized bed, Heat Transfer Engineering, Vol. 8, No. 4, p. 26.
10. Tianqing, L., 1995, Mechanism study on circulating flow of particles within a fluid bed antifouling heat exchanger, Proc. of Fouling

Mitigation of Industrial Heat Exchange Equipment, An International Conference, San Luis Obispo, California, pp. 377-384.

11. Lee, Y. P., Yoon, S. Y., Jurng, J. S. and Kim, N. H., 1995, Mechanism of fouling reduction and heat transfer enhancement in a circulating fluidized bed heat exchanger, Korean Journal of Air-Conditioning and Refrigeration Engineering, Vol. 7, No. 3, pp. 450-460.

12. Lee, K. B., Jun, Y. D. and Park, S. I., 2000, Measurement of heat transfer rates and pressure drops in a solid particle circulating fluidized heat exchanger, Korean Journal of Air-Conditioning and Refrigeration Engineering, Vol. 12, No. 9, pp. 817-824.

13. Jun, Y. D., Lee, K. B., Kim, A. K. and Lee, Y., 2002, Heat transfer characteristics and pressure drop of a fluidized bed heat exchanger without baffle plate, Korean Journal of Air-Conditioning and Refrigeration Engineering, Vol. 14, No. 2, pp. 989-995.

14. Kim, T. K., Youn, H. K., Seung, S. S. and Park, S. W., 2002, Development of a simulation software for the fluidized bed sludge incinerator, Proc. of KSME Autumn Annual Meeting, pp. 2179-2184.

15. Chun, W. P., Lee, K. W., Park, K. H., Lee, K. J. and Hwang, H. W., 2002, Heat transfer characteristics of organic sludge particles in rotary dryer, Proc. of KSME Autumn Annual Meeting, pp. 2185-2190.